Implementing the Results of Ventilation Research
16th AIVC Conference, Palm Springs, USA
19-22 September, 1995

The Combined Use of CFD and Zonal Modelling Techniques to Aid the Prediction and Measurement of Ventilation Effectiveness Parameters

M W Simons, J R Waters, J Leppard

School of the Built Environment, Coventry University, Priory Street, Coventry, UK

1 Synopsis

In order that sampling points may be strategically located, it is desirable to have knowledge of the spatial variation of ventilation effectiveness parameters prior to measuring them using tracer gas sampling techniques. The research described in this paper is being carried out to establish a tracer gas sampling strategy as well as to facilitate the prediction of ventilation effectiveness parameters.

The procedure developed requires the division of the internal space into a large number of cells and, by the application of CFD, the mass flow rates between adjacent cells to be established. Software developed at the University to predict interzonal flows has now been interfaced with the CFD software allowing the ventilation effectiveness parameters within each cell of the CFD model to be established.

Investigation of the computed values of the parameters reveals that the characteristics of many adjacent zones are almost identical. A method has been developed to combine small adjacent zones possessing similar characteristics thus allowing the model to be reduced to one of a small number of zones each possessing significantly different properties.

It is demonstrated in this paper that, in the simple mechanically ventilated buildings to which the research has at present been restricted, it is possible to produce reliable contour diagrams of ventilation parameter variations from a small number of properly defined large zones. The large zones found in this way may be used both as a guide to the location of tracer gas sampling points and as the basis of a simplified model for design calculations.

2 List of Symbols

Symbol		Units
ε^c	contaminant removal effectiveness	
ε_p	local air change index at point p	
ε_p^c	local air quality index at point p	
$\bar{\tau}_p$	local mean age of air at point p	s
τ_n	nominal time constant	s

3 Introduction

The measurement of ventilation effectiveness parameters requires the injection of tracer gas followed by sampling of the air at various points within the space. However, physical limitations imposed by the equipment used for this work restricts measurement to a relatively small number of points. It is essential therefore that sampling points are selected carefully in order that when the ventilation parameters are measured, they reflect the air movement characteristics of the whole of the space under consideration. This work represents a development of that reported by MW Simons etal [1].

4 Ventilation Effectiveness Parameters

4.1 The most commonly used measures of ventilation, air change rate, and its reciprocal the nominal time constant, τ_n, share the disadvantage of relating to the whole space and not reflecting the variability of air movement within the space. This may be overcome by the use of Ventilation Effectiveness Parameters which may be categorised as follows:

Air change efficiency, which is a measure of how effectively the air present in the room is replaced by fresh air from the ventilation system, and

contaminant removal effectiveness, which is a measure of how quickly a contaminant is removed from a room.

The above parameters are described in detail in the AIVC Technical Reports 28,[2] and 28.2,[3] respectively. A brief explanation of the parameters relevant to this report follows.

4.2 Air Change Efficiency

(I) Local Mean Age of Air, $\bar{\tau}_p$

Local mean age is defined as the average time it takes for air to travel from the inlet to any point p in the room, and may be written as:

$$\bar{\tau}_p = \int_0^\infty t.A_p(t).dt$$

where $A_p(t)$ represents the age distribution curve for air arriving at point p. The local mean age of the air is different for all points, p within the room.

(ii) Local Air Change Index, ε_p

This index characterises the age of air at a point relative to the overall supply rate and is defined as:

$$\varepsilon_p = \frac{\tau_n}{\bar{\tau}_p}$$

It will be seen that the lower the local mean age of air at a point, then the better will be the supply of fresh air to that point whereas a value of local air change index greater than 1 indicates that the point in question is receiving air more efficiently than the average.

4.3 Contaminant Removal Effectiveness

(i) Local Air Quality Index, ε_p^c

Local air quality index is defined as the ratio between the steady state concentration of contaminant at the exhaust duct and the steady state concentration of contaminant at point p in the room.

$$\varepsilon_p^c = \frac{C_e(\infty)}{C_p(\infty)}.$$

Since contaminant may be injected anywhere within the room, for a point p, there are an infinite number of values depending on the location of the source.

(ii) Contaminant removal effectiveness, ε^c

Contaminant Removal Effectiveness is defined as the ratio between the steady concentration of contaminant at the exhaust duct and the steady state concentration of the room.

$$\varepsilon^c = \frac{C_e(\infty)}{< C(\infty) >}$$

This index gives an average performance for the whole room but its value also depends on the location of the contaminant source and hence there are also an infinite number of possible values.

Large values of Local Air Quality Index or Contaminant Removal Effectiveness are indicative of efficient removal of contaminant.

5 Experimental Strategy

5.1 The approach adopted was to select a simple mechanically ventilated space at Coventry University which, following predictive analysis, could be used for corroborative physical measurements. The room chosen was approximately rectangular with dimensions of 5.04m x 4.62m x 2.70m and is shown in Figure 1. Initially CFD analysis was undertaken to establish interzonal air flow rates having first set up a relatively fine grid consisting of 1664 cells. The results of this initial analysis are shown graphically in Figure 1.

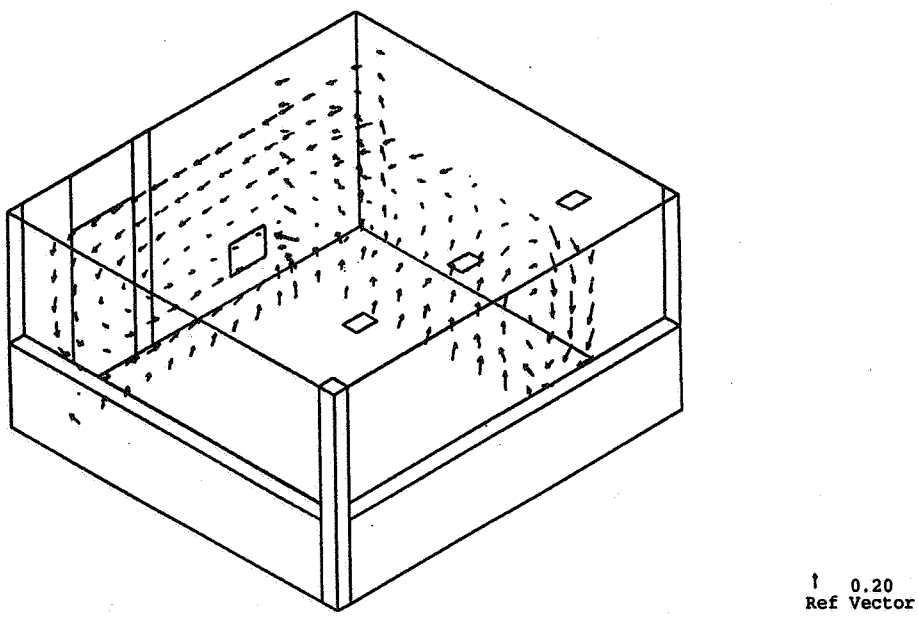

Figure 1 Air movement Pattern (Initial Model)

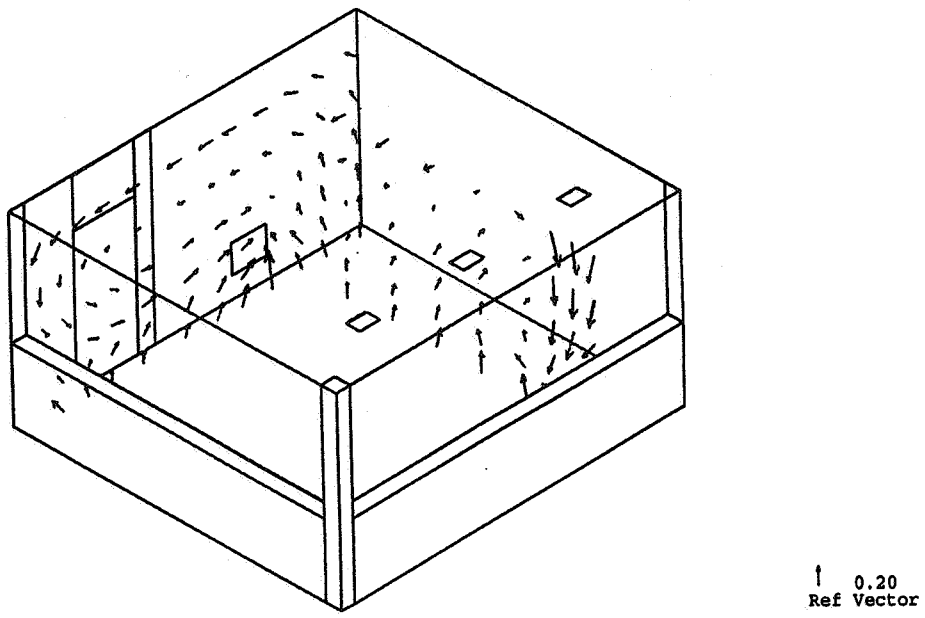

Figure 2 Air movement Pattern (Following First Cell Reduction)

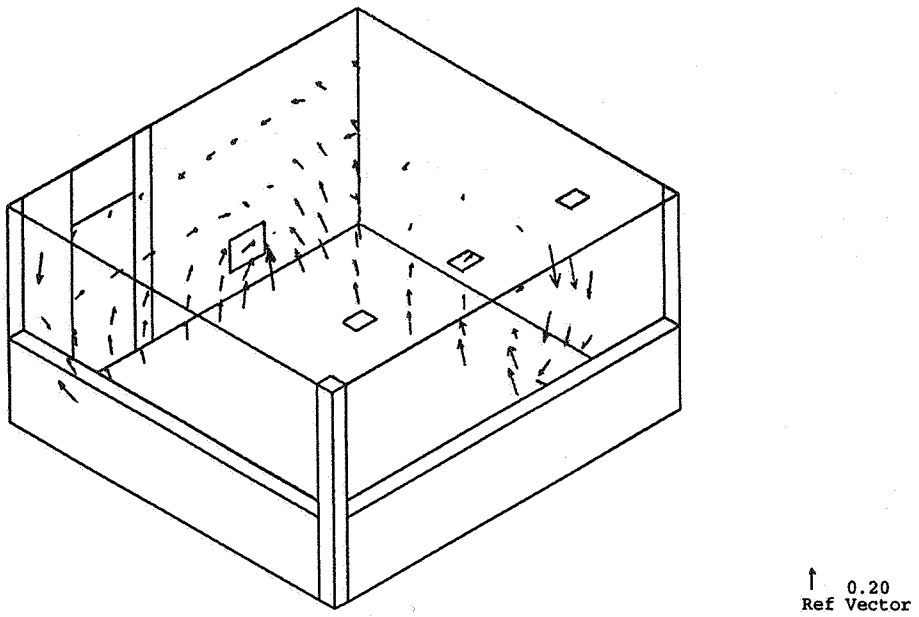

Figure 3 Air movement Pattern (Following Second Cell Reduction)

Since the objective was to reduce the space to a small number of measurement zones, the CFD was repeated for increasingly coarser grids whilst ensuring that the overall air flow pattern within the room remained unchanged. The result of this crudification can be seen in Figures 2 and 3. The latter, which consisted of a 5 x 8 x 11 grid of 440 cells, produced an essentially similar velocity vector pattern as the 1664 cell model, and was therefore used as the basis of the subsequent analysis. Studies have been carried out using a variety of mass flow rates. In this paper the results of a case where the mass flow rates at the 3 inlets were 0.114,0.117 and 0.145 kg/s with inlet air velocities of 1.89,1.95 and 2.42 m/s respectively is considered.

5.2 The ventilation effectiveness and contaminant removal effectiveness parameters can, in principle, be obtained by means of the CFD model. One way of doing this is to inject a contaminant at a suitable location and allow the model to compute the equilibrium concentrations throughout the space. These equilibrium concentrations may then be used to find the desired parameter. However, it is more efficient to convert the velocity vectors found by the CFD model to interzone flow rates, and hence produce the inter zone flow matrix of the of the equivalent multizone model of the problem. All the ventilation parameters may then be found by manipulation of this flow matrix. Furthermore, the equivalent multizone model can be simplified (i.e. "crudified") down to a much smaller number of zones than would be possible with a CFD model.

5.3 The CFD software used for the analysis was 'Flovent' by Flomerics, which does not provide output of interzonal flow data. However, additional software was made available from Flomerics to provide this data, and a conversion algorithm has been written to convert this data to the interzonal matrix of the equivalent multizone model. Unfortunately, the CFD model operates over an overall grid which includes cells of solid material. These cells appear as zones of zero air movement in the multizone model, and so a facility has been included in the conversion algorithm to remove these dead zones. The final flow matrix, after conversion and removal of dead zones, becomes the input to existing software at Coventry University which computes all of the ventilation effectiveness parameters and contaminant removal parameters.

5.4 In order to reduce the number of zones in the above model it has been necessary to establish a strategy for merging zones, i.e. for crudifying the model. The strategy adopted has been to select an appropriate parameter, e.g. local air change index, and combine adjacent zones which have similar values of the index.

The method is to divide the indices into a number of contour bands of appropriate intervals. This may be done by setting an equal band width in which case the number of zones within each band is not equal or by adjusting the band width to ensure an approximately equal number of zones within each band. The merged zone model has a smaller number of zones and hence a smaller interzonal flow matrix which is then used to recompute the ventilation effectiveness parameters.

Results have been obtained for the unmerged model consisting of 440 zones, as shown in Figure 3. Removal of dead zones, i.e. those occupied by solid material, reduced the 440 zone model to 384 zones, and this 384 zone model was subjected to four degrees of merger. In each case, the merging process was based on values of the local air change index. The values for the four cases were fitted into 9, 5, 4 and 3 bands, the band interval being selected in each case to ensure an approximately equal number of the original 384 zones in each band.

6 Consideration of Results

6.1 Figure 4 illustrates the values obtained from the 384 zone model of the local air change index in each of the zones within a section running the length of the room and situated between air inlet and extract grills. The differences between the high values of this parameter in the well ventilated part of this slice through the building and its low values in the central portion are clearly evident in this figure. The same information displayed in contour diagram form via Flovent is shown in Figure 5.

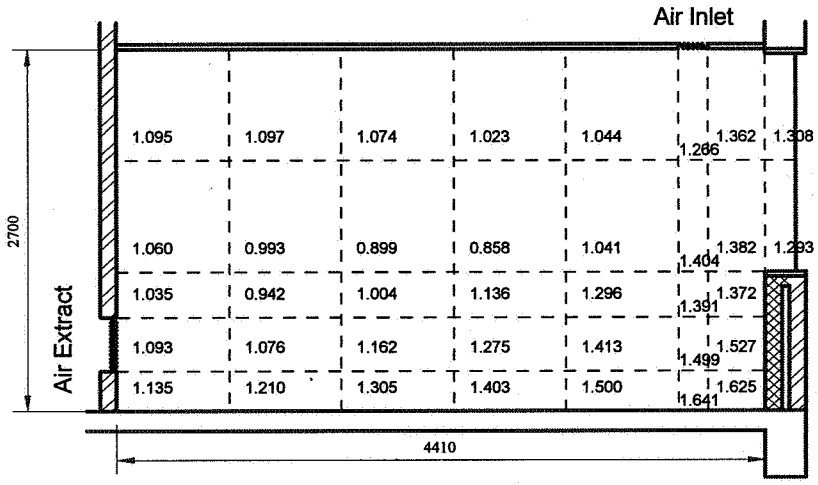

Figure 4 Local Air Change Index Within Each Zone

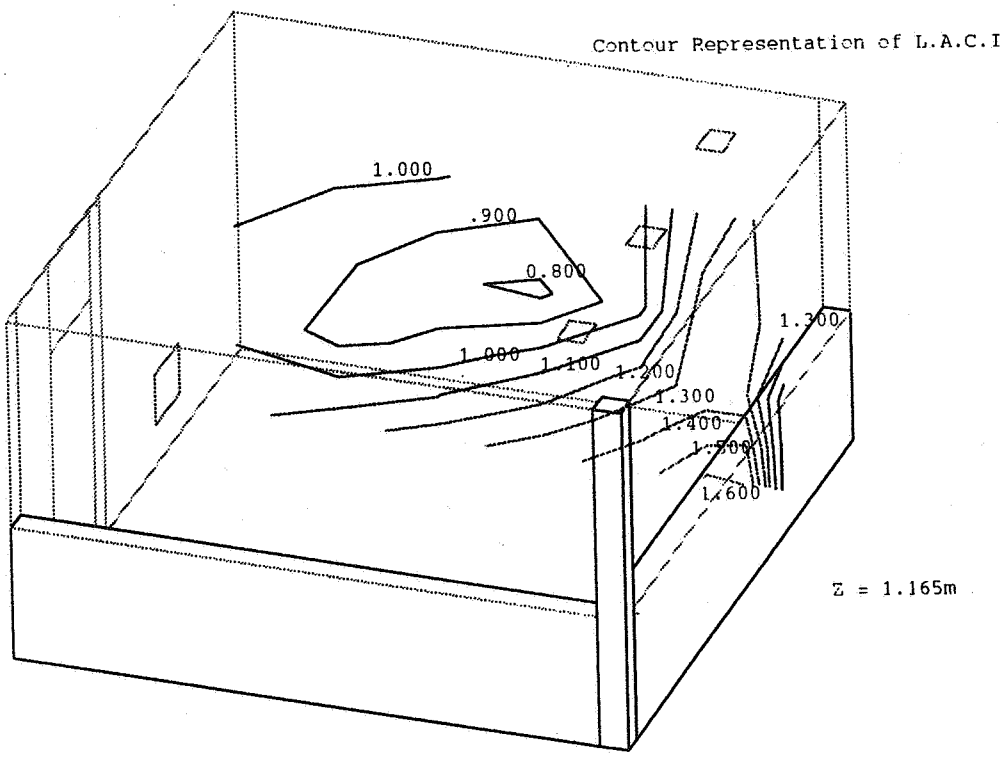

Figure 5 Contour Diagram Representation of Local Air Change Index Within Each Zone

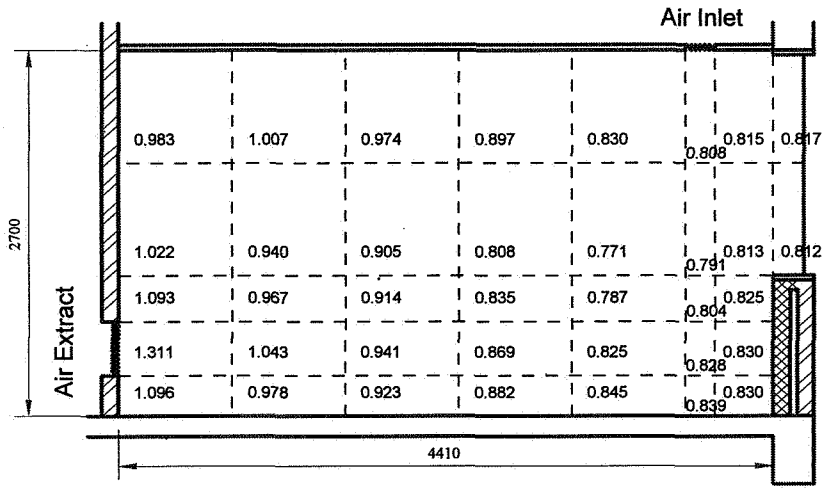

Figure 6 Contaminant Removal Effectiveness Within Each Zone

Figure 6 demonstrates variations in the contaminant removal effectiveness, i.e. how efficiently contaminant is removed from the whole room if subjected to injection into any one of the 37 cells within the slice of the room under consideration. This index of whole room performance indicates how much lower the concentration of contaminant would be if injection was close to the air extract, in which case much of the contaminant is removed directly with little or no circulation, compared with injection close to the inlet in which case contaminant is distributed efficiently throughout the whole space.

The above clearly demonstrate a technique whereby designers may predict spatial variations in ventilation effectiveness The values of a number of ventilation parameters in this and other sections of the space are shown in the poster display associated with this paper.

6.2 For the purposes of this report, zonal merger was based on the criterion of Local Air Change Index. Because of the relationship between Local Air Change Index and local Mean Age referred to in Section 4.2, it will be seen that analysis of the latter would have produced the same bands. Analysis could equally have been based on contaminant removal effectiveness, which would have produced different conclusions

The limits applied in the division into 9, 5, 4 and 3 bands are given below. This resulted in reductions from 384 to 88, 23, 15 and 5 zones respectively. It should be recognised that not all zones within each band are likely to be interconnected and hence it is always probable that the resulting number of zones will be greater than the number of bands into which the space has been divided.

The division of L.A.C.I. into bands for the current study was as follows;

9 bands		5 bands		4 bands		3 bands	
band limits	zones in band	band limits	zones in band	band limits	zones in band	band limits	zones in band
0.81		0.81		0.81		0.81	
	32		73		101		129
0.90		0.94		0.97		1.00	
	50		82		88		128
0.95		1.03		1.08		1.20	
	47		71		94		127
1.00		1.14		1.27		3.90	
	44		80		101		
1.05		1.35		3.90			
	33		78				
1.10		3.90					
	51						
1.20							
	49						
1.35							
	42						
1.60							
	36						
3.90							

The result of the subdivision is shown by way of block and contour diagrams in Figures 7 to 14. These clearly demonstrate how, as zonal reduction takes place:

(I) zones of similar Local Air Change Index are drawn together;

(ii) the basic pattern of the contour lines is retained; and

(iii) as would be expected, merger of the zones results in elimination of the highest and lowest values of the parameter when these are recalculated since the drawing together of similar values produces a result approaching the mean of its component parts.

The latter point is also clearly shown in Figure 15, where the value of Local Air Change Index based on the merged and unmerged cases are plotted for each of the original 37 occupied cells in the Section through the building shown in Figures 7 to 14. Figure 15 also serves to show how the variations in Local Air Change Index are retained throughout the merger process justifying the use of the merged model for the purpose of tracer gas sampling point location strategy.

Key to Figures 7 to 10.
x.xx(yyy) represents local air change index(zone number)

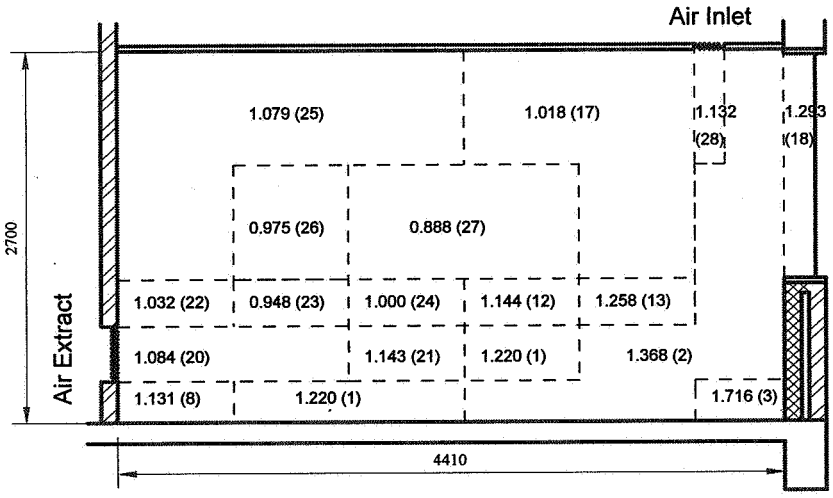

Figure 7 L.A.C.I. Following Reduction to 88 zones

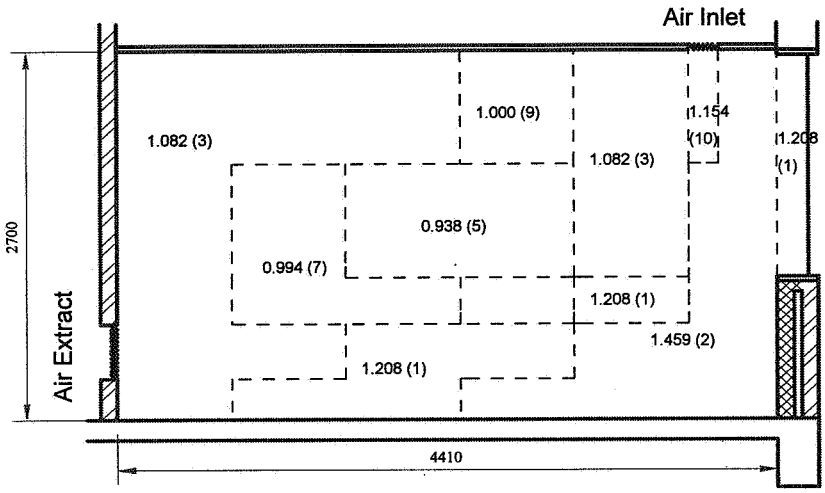

Figure 8 L.A.C.I. Following Reduction to 23 Zones

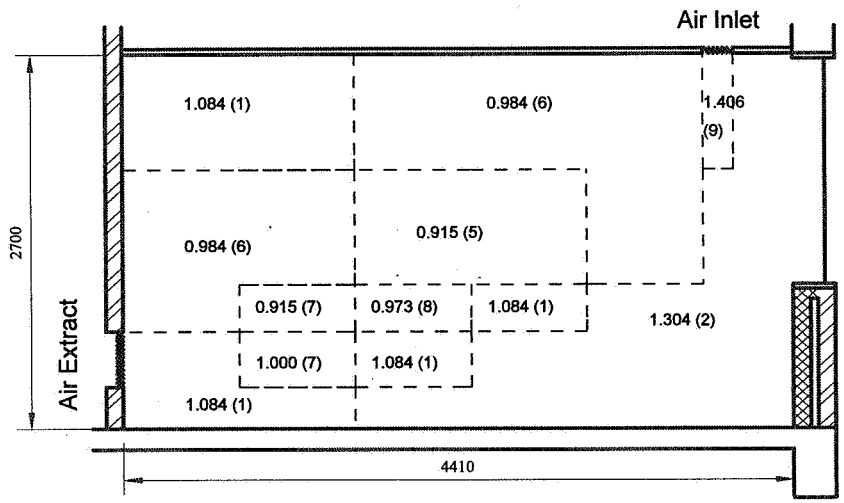

Figure 9 L.A.C.I. Following Reduction to 15 Zones

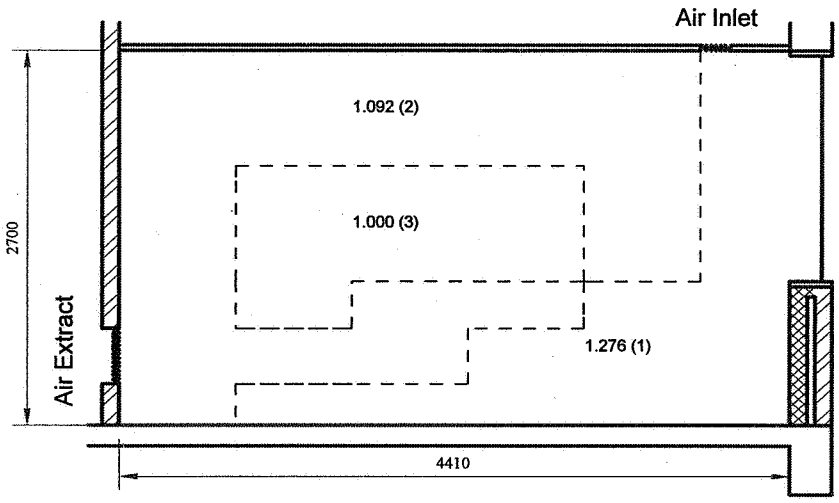

Figure 10 L.A.C.I. Following Reduction to 5 Zones

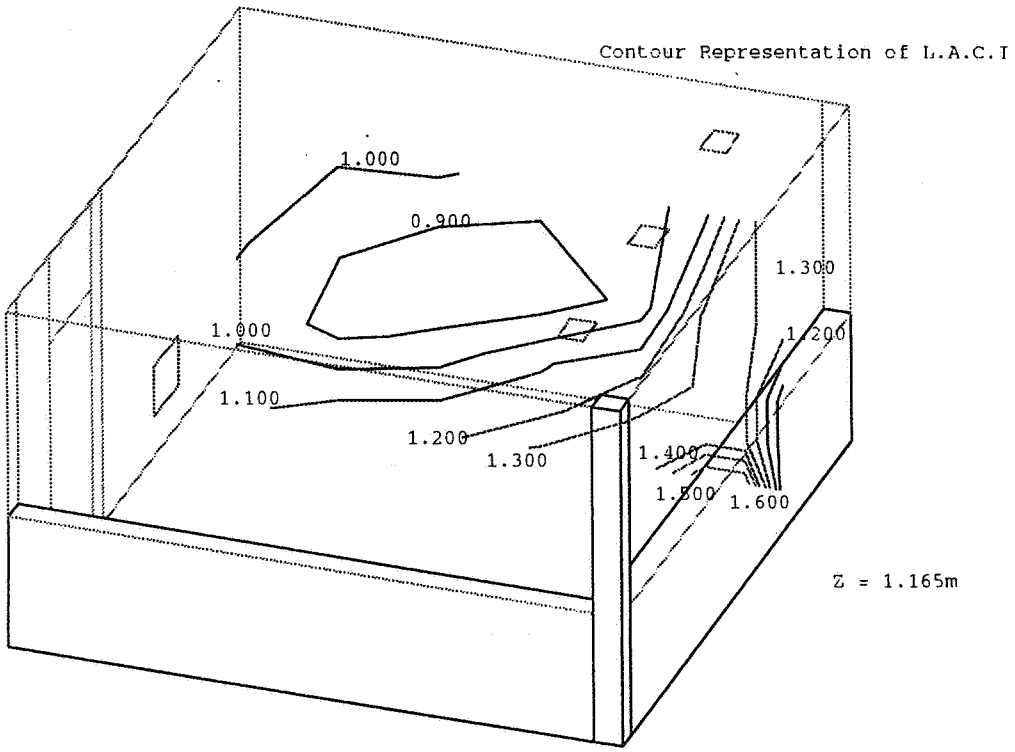

Figure 11 Contour Diagram of L.A.C.I. Following Reduction to 88 Zones

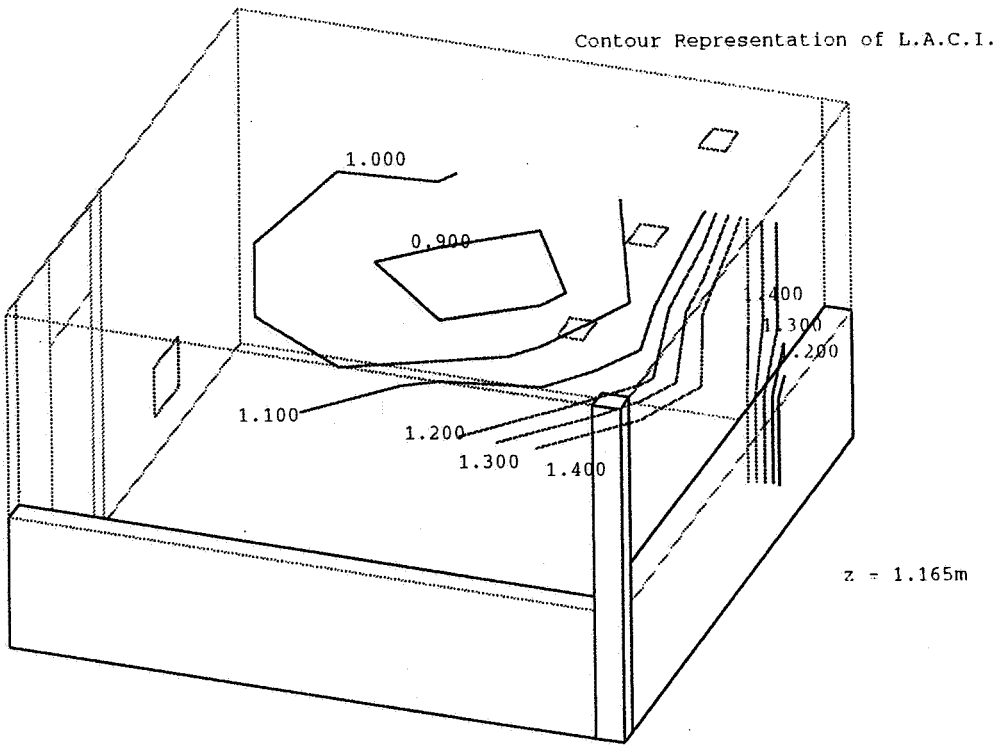

Figure 12 Contour Diagram of L.A.C.I. Following Reduction to 23 Zones

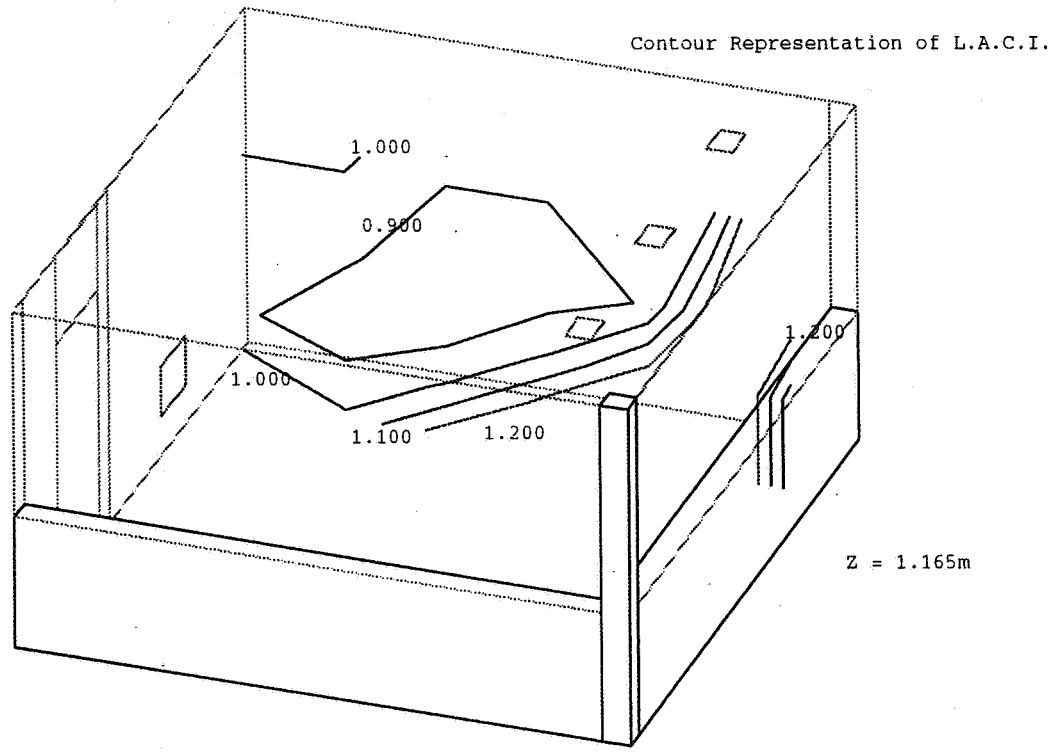

Figure 13 Contour Diagram of L.A.C.I. Following Reduction to 15 Zones

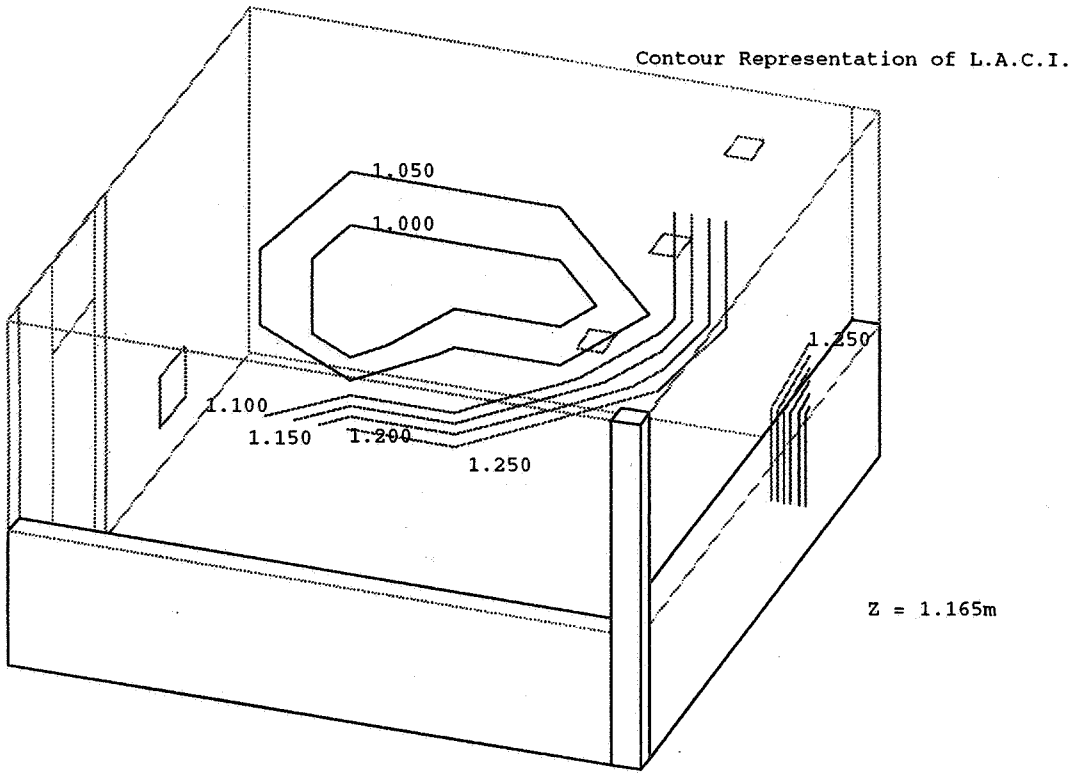

Figure 14 Contour Diagram of L.A.C.I. Following Reduction to 5 Zones

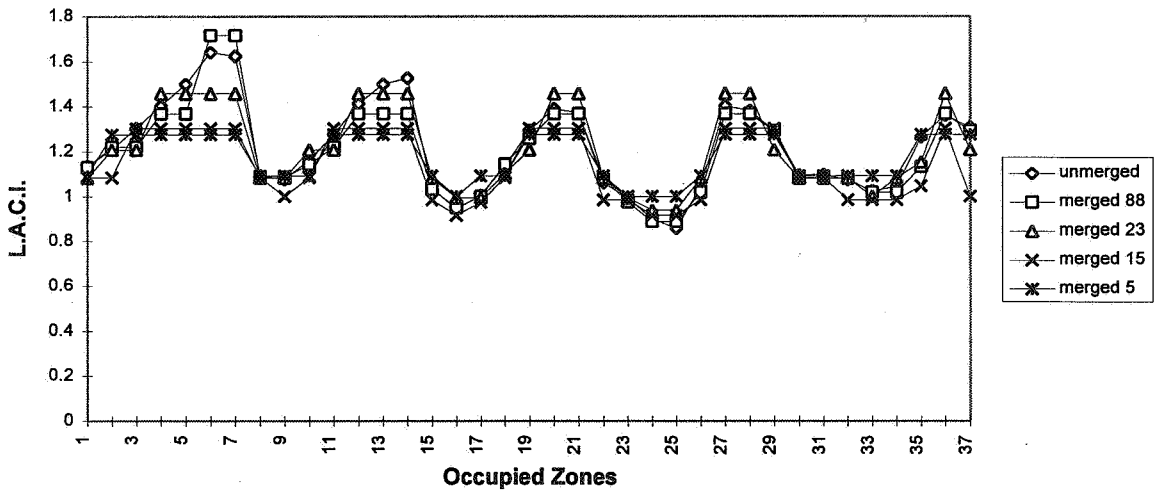

Figure 15 Variations in Initial and Merged Case Values of L.A.C.I.

7 Conclusions

Algorithms have been written to convert the output of a typical CFD model to an equivalent multizone model, which may then be used to compute all the usual ventilation effectiveness parameters. An additional algorithm has been written to reduce or "crudify" the multizone model to a smaller number of zones using any one of the ventilation effectiveness parameters as the criterion. Application of these algorithms to the computation of air movement in a typical mechanically ventilated room show that, in this case, a 384 zone representation of the space can be reduced to as little as a 5 zone representation without undue distortion of the computed values.

References

1 SIMONS, M.W., BROUNS, C.E. and WATERS, J.R.
'Flovent as an Aid to the Measurement of Air Movement Characteristics in Buildings'
Flovent User Meeting, May 1994

2 SUTCLIFFE, H.C.
'A Guide to Air Change Efficiency'
AIVC Technical Report 28, 1990

3 BROUNS, C.E. and WATERS, J.R.
'A Guide to Contaminant Removal Effectiveness'
AIVC Technical Report 28.2, 1991